

Strontium isotope variations in the lower Mississippi River and its estuarine mixing zone

Yingfeng Xu¹, Franco Marcantonio*

Department of Earth and Environmental Sciences, Tulane University, New Orleans, LA 70118, United States

Received 19 September 2006; received in revised form 5 January 2007; accepted 5 January 2007

Available online 18 January 2007

Abstract

The spatial and temporal variations of elemental and isotopic Sr in the Mississippi River (MR) mixing zone are examined in an attempt to address the extent to which estuarine environments modify the fluvial Sr flux on its way to the ocean. We collected samples from the MR delta and its outflow region during four cruises that took place from 1999 to 2002. MR discharge varied from about 7600–30,600 m³ s⁻¹. Mixing patterns revealed minimal non-conservative behavior of Sr in the dissolved pool. Monthly measurements of the Lower MR at an anchored site during 2000 shows that Sr input to the Gulf of Mexico from the MR varies temporally in both elemental concentration and isotopic composition, and that the flux of Sr is largely a function of water discharge. The extent of the non-conservative geochemical behavior of Sr does not compromise the use of Sr isotope ratios for stratigraphic dating purposes.

© 2007 Elsevier B.V. All rights reserved.

Keywords: Strontium; ⁸⁷Sr/⁸⁶Sr; Spatial; Temporal; Mississippi River; Gulf of Mexico

1. Introduction

At any given time, the world's ocean is isotopically uniform with respect to Sr. This is because Sr has a long residence time ($2-5 \times 10^6$ a) compared to the short mixing time ($\sim 10^3$ a) of water in the ocean (Brass, 1976; Burke and Denison, 1982; Carpo and DePaolo, 1990; McArthur, 1991; Henderson et al., 1994). Therefore, biogenic and authigenic marine precipitates

that have formed synchronously at different places in the world's ocean should incorporate Sr of the same isotopic signature. Measurements of the ⁸⁷Sr/⁸⁶Sr isotope ratio of these precipitates reveal past ocean Sr isotope variability, which can be an important tool for correlating and/or dating marine sequences (Burke and Denison, 1982; McKenzie et al., 1988; McArthur, 1994; Patterson et al., 1995; Veizer et al., 1997; Vaiani, 2000). Most of the observed changes in the Sr isotope ratio of the ocean through time are caused by changes in the relative contributions of hydrothermal exchange at ocean ridges versus weathering of rocks on the continents (Palmer and Edmond, 1989; Edmond, 1992). Hence the evolutionary history of the Sr isotope composition of the ocean may yield important information on global tectonic and/or climate change events (Burke and Denison, 1982; Aberg and Wickman, 1987;

* Corresponding author. Present address: Department of Geology and Geophysics, Texas A&M University, College Station, TX 77843, United States.

E-mail address: marcantonio@geo.tamu.edu (F. Marcantonio).

¹ Present address: National High Magnetic Field Lab, FSU, Tallahassee, FL.

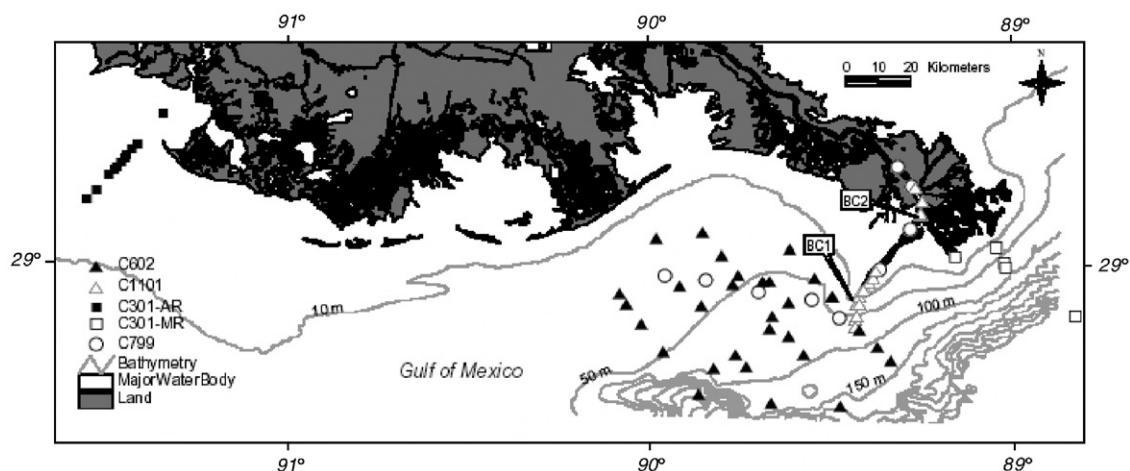


Fig. 1. Location map showing study area and sampling sites. Solid triangles denote samples collected during June 2002 (C602), open triangles denote samples collected during November 2001 (C1101), solid squares denote samples collected in March 2001 from the Atchafalaya River (C301AR), open squares denote samples collected in March 2001 from the Mississippi River (C301MR), open circles denote samples collected in July 1999 (C799).

Albarede and Michard, 1987; Raymo, 1991; Andersson et al., 1994; Derry and France-Lanord, 1996; Denison et al., 1998; Harris et al., 1998; Huh and Edmond, 1998).

Small but considerable regional differences in both flux and isotopic composition of Sr can occur on timescales shorter than its residence time in the ocean (Andersson et al., 1994; Derry and France-Lanord, 1996; Stoll and Shrag, 1998; de Villiers, 1999). In addition, in shallow marine environments, the riverine influence on Sr isotope systematics may result in deviations of the $^{87}\text{Sr}/^{86}\text{Sr}$ isotope ratio from that of contemporaneous seawater (Vaiani, 2000). Fully understanding the geochemical behavior of Sr in the riverine and estuarine environments may help to con-

strain interpretations of the past marine Sr budget in terms of variable erosional flux and global silicate weathering.

Detailed studies of the biogeochemistry of Sr in estuaries are rare. In the mixing zone of the Mississippi River (MR), the seventh largest river in the world with respect to both water and suspended sediment discharges (Meade, 1996), there has been only one estuarine spatial study of Sr geochemistry of which we are aware (Andersson et al., 1994). Our goal here is to contribute to the understanding of the geochemical behavior of Sr in estuarine environments by studying the mixing zone of the MR. Our objective is to establish the spatial and temporal variability of elemental and isotopic Sr within the MR mixing zone, and to

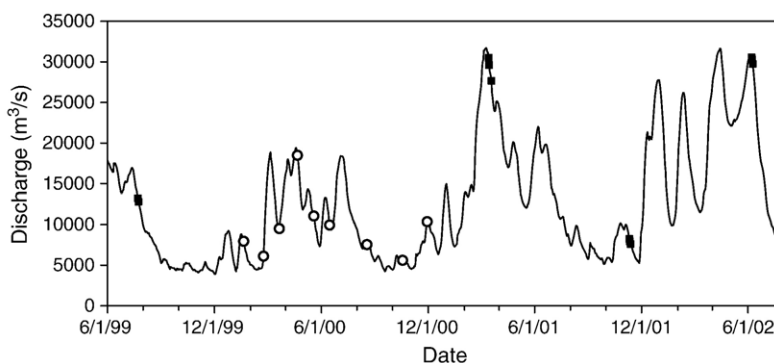


Fig. 2. Discharge at Tarbert Landing, Mississippi (from US Army Corps of Engineers website: <http://www.mvn.usace.army.mil/eng/edhd/watercon.htm>). This site is approximately 500 km upstream from the mouth of the Mississippi River at SW Pass. Solid squares indicate the timing of cruise sampling, while open circles indicate the timing of monthly Mississippi River sampling at New Orleans.

Table 1
Sr concentration and isotopic composition of dissolved load for water collected during four different discharge periods

Cruise	Sample	LNG ^a	LAT ^b	Salinity	SPM ^c	Sr ($\mu\text{mol/kg}$) ^d	⁸⁷ Sr/ ⁸⁶ Sr ^e		
C799	Surface	–89.2910	29.2597	0.0	120.2	2.13	0.70957		
		–89.2848	29.2042	0.0	118.2	2.13	0.70959		
		–89.2908	29.0857	0.1	104.1	2.45	0.70953		
		–89.3715	28.9738	1.5	54.0	9.69	0.70924		
		–89.4857	28.8402	4.8	11.6	41.52	0.70917		
		–89.5597	28.8918	18.5	9.7	39.69	0.70919		
		–89.7060	28.9145	16.4	15.2	41.93	0.70917		
		–89.8537	28.9450	16.7	14.2	43.67	0.70918		
		–89.9663	28.9583	15.7	17.3	51.97	0.70918		
	Bottom	–89.2910	29.2597	0.2	363.7	2.21			
		–89.2848	29.2042	0.2	228.4	2.24	0.70959		
		–89.3715	28.9738	35.6	17.7	89.61	0.70915		
		–89.4857	28.8402	36.4	5.9	94.19	0.70916		
		–89.5597	28.8918	36.3	9.2	92.89	0.70914		
		–89.8537	28.9450	36.0	7.5	92.05			
		–89.9663	28.9583	35.9	6.8	85.33	0.70914		
		C301-MR	Surface	–89.1668	29.0093	0.1	334.0	1.43	0.70997
				–89.0525	29.0336 ^f	1.9	119.0	5.93	0.70933
				3.0	53.3	8.19	0.70928		
				14.0	20.0	41.08	0.70915		
–89.0272	28.9822			19.1	26.0	54.60	0.70913		
–89.0300	28.9922			19.5	38.0	50.63	0.70917		
–88.8347	28.8461 ^f			21.5	14.7	60.26	0.70913		
				26.5	24.7	68.56	0.70914		
C301-AR	Surface	–91.3540	29.4056	0.0	162.0	1.43	0.70998		
		–91.4257	29.3233	0.1	110.0	1.96			
		–91.4398	29.3074	2.1	86.0	6.47			
		–91.4548	29.2925	4.1	66.0	11.81			
		–91.4603	29.2842	6.1	39.0	16.77	0.70916		
		–91.4711	29.2710	8.1	32.7	22.47			
		–91.4830	29.2587	10.1	24.7	26.36			
		–91.4909	29.2511	12.0	21.3	32.74			
		–91.5038	29.2352	15.6	22.7	40.70			
		–91.5380	29.1968	19.9	24.7	53.65			
		–91.5656	29.1672	26.0	24.4	70.19			
C1101	Surface	–89.4390	28.8150	22.3	15.4	53.75			
		–89.4350	28.8470	22.2	14.3	50.25			
		–89.4280	28.8800	18.2	11.6	44.84			
		–89.4180	28.9200	6.4	15.1	16.95			
		–89.4290	28.9010	14.2	14.7	36.16			
		–89.4250	28.9140	7.7	17.1	19.94			
		–89.4150	28.9230	6.8	17.2	17.17			
		–89.4030	28.9380	5.8	13.9	15.11			
		–89.3930	28.9530	4.4	15.2	17.36			
		–89.3820	28.9700	3.0	13.1	9.29			
		Bottom	–89.4390	28.8150	35.8	7.8	82.60		
	–89.4350		28.8470	35.7	11.6	83.29			
	–89.4280		28.8800	35.6	14.5	82.26			
	–89.4180		28.9200	35.1	21.0	82.87			

Table 1 (continued)

Cruise	Sample	LNG ^a	LAT ^b	Salinity	SPM ^c	Sr ($\mu\text{mol/kg}$) ^d	⁸⁷ Sr/ ⁸⁶ Sr ^e
C602	Surface	-89.5518	28.9510	12.2	15.5	34.97	0.709158
		-89.5044	28.8983	4.3	19.7	12.50	0.709243
		-89.4267	28.8067	7.4	13.1	23.40	0.709182
		-89.3792	28.7571	3.0	17.8	6.53	0.709340
		-89.4810	28.5919	31.0	6.2	81.85	0.709138
		-89.8315	28.6967	15.1	11.2	34.01	0.709159
		-89.5824	28.7350	13.3	13.8	39.37	0.709154
		-89.6237	28.7865	10.5	7.8	29.49	
		-89.7625	28.9585	12.9	11.8	34.97	0.709161
		-89.8093	29.0160	12.0	8.9	34.00	0.709158
		-89.8606	29.0793	11.8	12.1	34.26	
		-89.9896	29.0583	25.7	11.3	69.63	
		-89.8637	28.8723	36.5	8.8	95.35	
		-89.7702	28.7402	24.0	8.6	66.35	
		-89.7397	28.7004	33.2	12.6	88.05	
		-89.8724	28.6270	36.4	1.6	97.72	
		-89.9713	28.7477	36.5	1.5	96.96	
		-90.0912	28.9076	34.5	11.2	90.93	
		-89.9247	28.9282	35.6	2.7	91.59	
		-89.6967	28.9375	13.7	9.4	38.36	
		-89.6774	28.9386	11.0	10	31.01	
		-89.6235	28.8839	3.8	20	10.41	
		-89.6776	28.8123	25.4	7.6	77.81	
	MR			0.0	35.4	1.57	0.71009
	SW	-89.6712	28.6040	36.5	2.8	97.99	0.70912
C602-6	1.5 m	-89.8596	29.0883	12.2	9.6	37.70	0.70917
	19 m			36.5	15.4	95.46	0.70915

a. longitude, negative sign indicates West; b. latitude, North; c. suspended particulate matter concentration in mg/l; d. $\pm 4\%$ (based on reproducibility of replicate analyses); e. $\pm 0.001\%$ (based on reproducibility of laboratory standards and replicate analyses of samples); f. samples taken at different salinities in the water column of the same site.

determine the extent to which Sr displays non-conservative behavior.

2. Sampling and analytical methods

From the MR and its outflow region in the Gulf of Mexico (GOM), we sampled dissolved ($<0.2 \mu\text{m}$), particulate ($>0.2 \mu\text{m}$), and sedimentary phases during four cruises that spanned the four-year period of 1999 to 2002 (Fig. 1). The timing of each cruise was representative of low-, intermediate-, or high-water discharge periods (solid squares in Fig. 2). In July 1999, an intermediate discharge period, surface ($\sim 4 \text{ m}$ below water surface; bws) and bottom waters were sampled from Southwest (SW) Pass, a distributary of the MR, and from the outflow region west of SW Pass (Fig. 1). During March 2001, a high discharge period, surface water ($\sim 1 \text{ m}$ bws) samples were collected from the outflow region of South Pass, another distributary in the bird's foot delta of the MR (Fig. 1). During the November 2001 low discharge period, surface ($\sim 1\text{--}2 \text{ m}$ bws) and water depth profile samples were collected from SW Pass, and from

the outflow region south of SW Pass (Fig. 1). During June 2002, a high discharge period, surface ($\sim 1\text{--}3 \text{ m}$ bws) and deep waters were sampled from the outflow region south and west of SW Pass (Fig. 1). The salinities encountered in all waters sampled ranged from 0.04‰ to 36.5‰ .

Surface water ($\sim 1 \text{ m}$ bws) was sampled in the outflow region of the Atchafalaya River (AR) during the March 2001 cruise. The AR captures 30% of the MR discharge in addition to the flow of the Red River (Coleman et al., 1998) and empties into the GOM over a broad shallow outflow region. The AR and AR outflow region samples had salinities that range from $0\text{--}26\text{‰}$.

During 2000, in order to determine the temporal variations of Sr in fresh MR water, monthly sampling of river water was conducted on the US Army Corps of Engineers Dock in New Orleans (open circles in Fig. 2). Surface water ($\sim 1 \text{ m}$ bws) was sampled for dissolved and particulate phases.

Water samples from July 1999 and water depth profile samples from June 2002 were obtained from NiskinTM bottles on a CTD-Rosette system. All samples from March 2001 and some from June 2002 were

collected with Teflon™ tubing connected to a multiple instrument data acquisition system (MIDAS). Samples from November 2001 were collected through nitric-acid-cleaned tubing, which was attached to a CTD system and driven by a peristaltic pump. Bottles used to collect samples were pre-cleaned with nitric acid and de-ionized (DI) water. Each bottle was washed three times on-site with sample water before sample collection. Salinity was determined by conductivity measurements using either the CTD or MIDAS systems. All samples were processed by vacuum filtering through 0.2- μm , 47-mm diameter polycarbonate membrane filters, usually within 1 hour after collection. Two aliquots were filtered

per sample. The filtrate from the second aliquot, after the filtration apparatus had been “well-conditioned” with sample water, was collected for analysis. The filtration apparatus was carefully rinsed with dilute nitric acid and DI water between samples. Dissolved (<0.2 μm) samples were stored in acid-cleaned and DI-water-rinsed bottles, and acidified to a pH of about 1 with ultrapure HNO_3 acid in order to stabilize the trace metals. Filters that contained the particulates (>0.2 μm) were stored in acid-cleaned, DI-water-rinsed holders. Particulate samples, after being transported back to the lab, were air-dried inside a 100-class clean laminar-flow hood at room temperature or dried at 40 °C inside an oven with the filter-holder lid loosely covered.

Solid samples were digested with ultrapure (Seastar™) HF and HNO_3 at approximately 140 °C. After digestion no residue was visible, and we assume that dissolution was complete. To minimize contamination, sample preparation, digestion, and purification were performed under Class 100 clean conditions. For elemental Sr concentration analysis, digested solid samples were diluted with ultrapure concentrated HNO_3 and DI water (2% solution). Elemental Sr concentrations were measured with the Finnigan Element 2 Inductively-Coupled Plasma Mass Spectrometer (ICP-MS) at Tulane University. Procedural Sr blanks, consistently less than 3% of analyte Sr, were applied. Sr concentration external reproducibility averaged about 3.9% for high-salinity samples (four triplicate analyses, Table 1), and about 2.5% for lower-salinity samples (five duplicate analyses; Xu, 2004). In addition to replicate Sr analysis, in order to monitor for matrix effects, high-salinity samples were run for Sr in conjunction with an open-ocean seawater standard from the National Research Council of Canada (CASS-4). Although this standard is not certified for Sr,

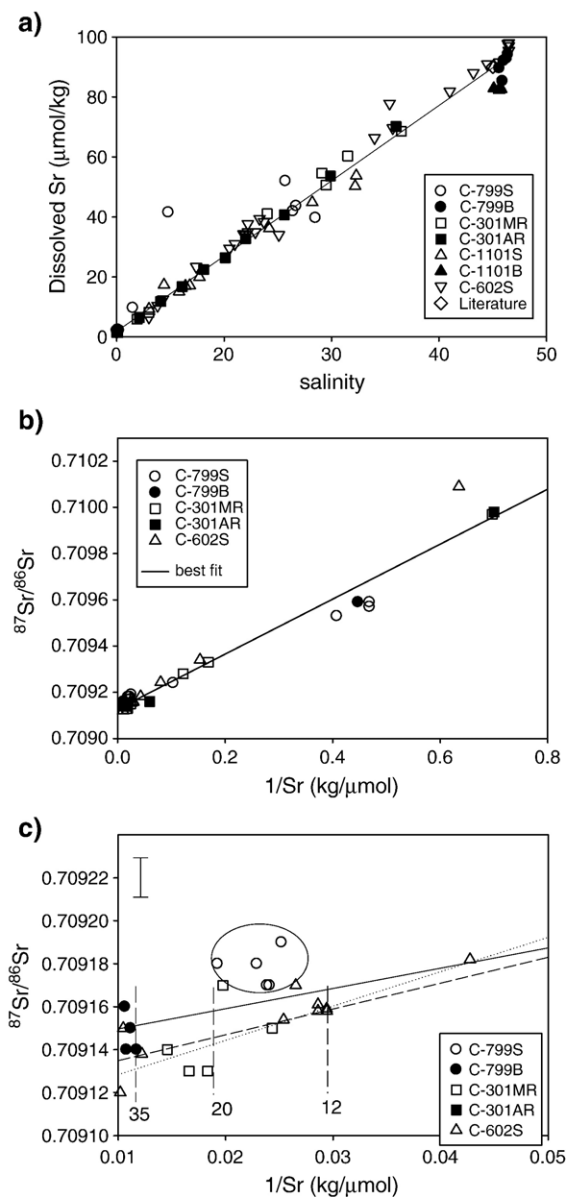


Fig. 3. a) Dissolved (<0.2 μm) Sr concentrations ($\mu\text{mol/kg}$) versus salinity (parts per mil, ‰). The line represents a tie-line between two endmembers: world ocean water (90 $\mu\text{mol/kg}$ at salinity of 35‰; de Villiers, 1999) and average data for MR water from this study (1.7 $\mu\text{mol/kg}$; 0‰). Suffixes in legend symbols refer to surface (S) and bottom (B) waters. b) Isotopic systematics of dissolved Sr in the Mississippi River mixing zone. The seawater endmember (diamond symbol) has a Sr concentration of 90 $\mu\text{mol/kg}$ and a $^{87}\text{Sr}/^{86}\text{Sr}$ isotope ratio of 0.70915 (Andersson et al., 1994; Goldstein and Jacobsen, 1987). The best-fit line for all of the data points has a correlation coefficient, r^2 , of 0.96. c) Sr isotope ratio versus Sr concentration for high-salinity samples (i.e., an expansion of Fig. 3b at the seawater endmember). Data points enclosed in the circle are those that contain Sr with anomalous Sr isotopic ratios (see text for discussion). Each line is a best-fit line for three separate cruises: solid line — July 1999, dashed line — March 2001, dotted line — June 2002). For July 1999, the best-fit line excludes the data points with anomalous Sr isotopic ratios. The error on Sr isotope ratio analyses is shown in the upper left corner of graph.

Table 2
Sr concentration and isotopic composition of particulate load in Mississippi River water collected during four different discharge periods

Cruise	Sample	LNG ^a	LAT ^b	Sr (mmol/kg) ^c	⁸⁷ Sr/ ⁸⁶ Sr ^d
C799	Surface	-89.2910	29.2597	1.56	0.71849
		-89.2848	29.2042	1.71	0.71854
		-89.2908	29.0857	1.42	0.71868
		-89.3715	28.9738	1.34	0.71824
		-89.4857	28.8402	2.56	0.71295
		-89.5597	28.8918	2.24	0.71029
		-89.7060	28.9145	3.98	0.70946
		-89.8537	28.9450	2.84	0.70933
		-89.9663	28.9583		0.70949
	Bottom	-89.2910	29.2597	1.51	
		-89.2848	29.2042	1.34	0.71842
		-89.3715	28.9738	1.62	0.71532
		-89.4857	28.8402	2.78	0.71336
		-89.5597	28.8918	2.00	0.71498
		-89.8537	28.9450	1.62	0.71304
		-89.9663	28.9583		0.71189
				2.65	
				1.34	
				1.40	
C301-MR	Surface	-89.1668	29.0093	1.31	
		-89.0525	29.0336	1.27	
				2.65	
				1.34	
		-89.0272	28.9822	1.40	
		-89.0300	28.9922	1.60	
		-88.8347	28.8461	1.55	
		1.44			
C301-AR	Surface	-91.3540	29.4056	1.56	
		-91.4257	29.3233	1.39	
		-91.4398	29.3074	1.59	
		-91.4548	29.2925	2.31	
		-91.4603	29.2842	1.67	
		-91.4711	29.2710	1.36	
		-91.4830	29.2587	1.56	
		-91.4909	29.2511	1.54	
		-91.5038	29.2352	1.47	
		-91.5380	29.1968	1.86	
		-91.5656	29.1672	1.57	
C1101	Surface	-89.428	28.880	1.81	
		-89.418	28.920	1.89	
		-89.429	28.901	2.08	
		-89.415	28.923	1.68	
		-89.393	28.953	1.71	
Bottom	-89.439	28.815	1.84		
	-89.428	28.880	1.65		
	-89.418	28.920	1.89		
C602	Surface	-89.5518	28.9510	3.74	
		-89.5044	28.8983	2.36	
		-89.4267	28.8067	1.57	
		-89.3792	28.7571	2.22	
		-89.4810	28.5919	2.20	
		-89.8315	28.6967	2.26	

Table 2 (continued)

Cruise	Sample	LNG ^a	LAT ^b	Sr (mmol/kg) ^c	⁸⁷ Sr/ ⁸⁶ Sr ^d
C602	Surface	-89.5824	28.7350	1.84	
		-89.6237	28.7865	2.31	
		-89.7625	28.9585	1.71	
		-89.8606	29.0793	1.48	
		-89.8637	28.8723	1.56	
		-89.7702	28.7402	2.26	
		-89.7397	28.7004	1.93	
		-89.8724	28.6270	2.12	
		-89.9713	28.7477	2.00	
		-90.0307	28.8202	2.31	
		-90.0912	28.9076	2.00	
		-89.9247	28.9282	2.20	
		-89.6967	28.9375	3.47	
		-89.6235	28.8839	1.61	
		-89.6776	28.8123	1.87	

^a Longitude, negative sign indicates West.

^b Latitude, North.

^c ±4% (based on reproducibility of replicate analyses).

^d ±0.001% (based on reproducibility of laboratory standards and replicate analyses of samples).

our measured Sr concentrations were within 1% of that expected assuming a conservative behavior for Sr in the open ocean.

For Sr isotope analysis, samples were purified by ion exchange chromatography using Sr-specific resin (Eichrom™) and measured by Thermal Ionization Mass Spectrometry (TIMS) at Florida State University and Louisiana State University (both using a Finnigan MAT 262). The average ⁸⁷Sr/⁸⁶Sr ratio of the Eimer and Amend Sr isotope standard (reference value: 0.70800) during the course of our study at FSU was 0.708007±0.000004 (2σ, n=15). The ⁸⁷Sr/⁸⁶Sr ratio of NBS987 (reference value: 0.71025) obtained during the course of our study at LSU was 0.710258±0.000009 (2σ; 1 analysis). Duplicate Sr isotope analyses of two surface water samples were performed (Table 1). One set of analyses was performed at LSU in 2003 and a duplicate set of the same samples was performed at FSU in 2004. The duplicate analyses, one year apart and at different laboratories, were indistinguishable from each other and within the “blanket” reproducibility of the Sr isotope standards (i.e., 0.001%).

3. Results

3.1. The distribution and isotopic composition of Sr in the water column of the MR mixing zone

3.1.1. Dissolved load

All of our Sr dissolved data (Table 1) generally follow a mixing line formed by “tying” two endmembers on a

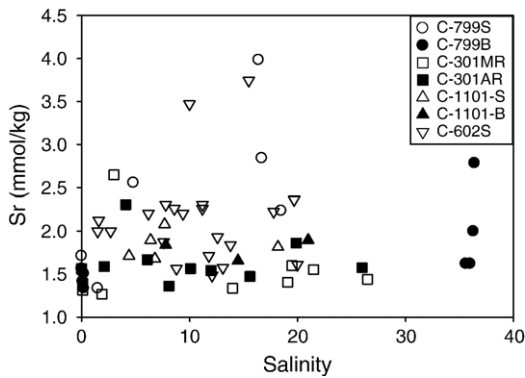


Fig. 4. Particulate ($>0.2 \mu\text{m}$) Sr concentrations (mmol/kg) versus salinity (parts per mil, ‰). Legend symbols are the same as those used in Fig. 3.

concentration-salinity plot (Fig. 3a). The endmembers are MR water ($1.7 \mu\text{mol/kg}$; average of our values; lower left) and world ocean surface water ($90 \mu\text{mol/kg}$; de Villiers, 1999; upper right). There is some scatter, and several points fall above or below the best-fit mixing line. Most of the data points that fall below the mixing line are representative of the high-salinity deep water samples from November 2001 (Fig. 3a; solid inverted triangles).

One data point that falls significantly above the mixing line, at a salinity of about 5‰ (Fig. 3a; open circle), represents a surface sample from the July 1999 cruise. It is possible that an anomalously sharp salinity gradient at this particular site ($\sim 25\text{‰/m}$) has compromised the salinity measurement.

In a plot of $^{87}\text{Sr}/^{86}\text{Sr}$ isotope ratio versus inverse Sr concentration (Fig. 3b), a linear correlation is evident (r^2 of 0.96 for all data points), with MR water and seawater forming the two endmembers of a binary mixing line. Data points are focused near the seawater endmember (lower left), characterized by low $^{87}\text{Sr}/^{86}\text{Sr}$ isotope ratios and high Sr concentrations. The MR endmember (upper right), with lower concentrations and higher $^{87}\text{Sr}/^{86}\text{Sr}$ isotope ratios, has much more scatter associated with it. Improved correlation coefficients are obtained if separate linear regressions are performed on the data from each cruise. Although the independent regressions for each cruise are not shown, the Sr isotope-concentration data from the July 1999 cruise are well correlated with an r^2 of 0.990, as are the March 2001 (r^2 of 0.999 when both MR and AR transects are included) and the June 2002 data (r^2 of 0.999). The differences in the slopes of the best-fit lines for each cruise are

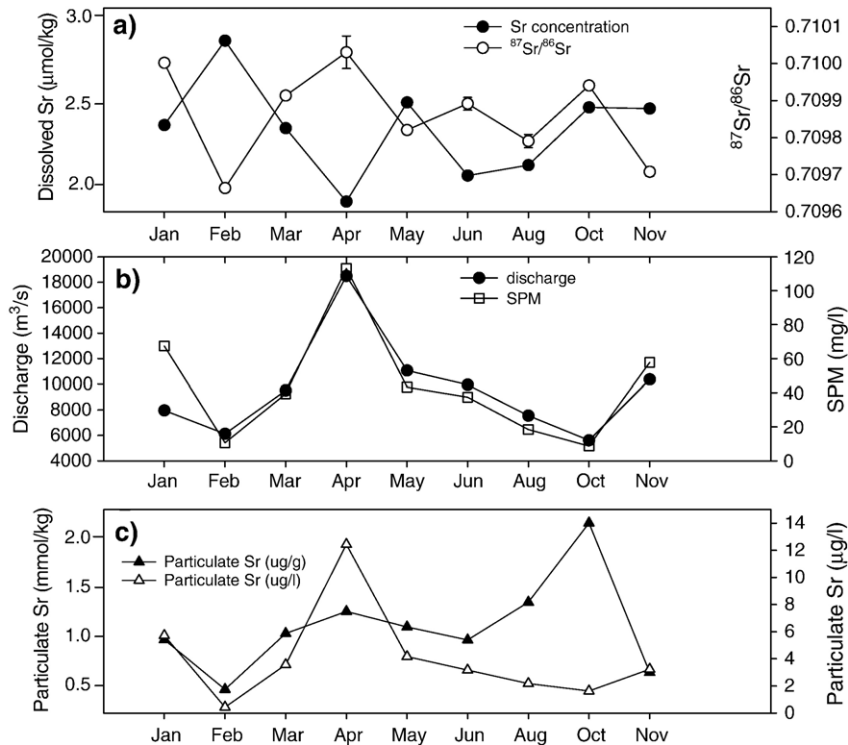


Fig. 5. Seasonal variability of elemental and isotopic Sr in the MR at New Orleans. a) dissolved ($<0.2 \mu\text{m}$) Sr concentration ($\mu\text{mol/kg}$) and $^{87}\text{Sr}/^{86}\text{Sr}$ isotope ratios; b) Water discharge (at Tarbert Landing, MS) and total suspended particulate matter (SPM); c) Sr content of particulate (mmol Sr/kg particulates) and particulate Sr content of water ($\mu\text{g Sr/L}$ water).

primarily derived from the changes in the river water endmember, which varies with respect to $^{87}\text{Sr}/^{86}\text{Sr}$ isotope ratio between about 0.7096 and 0.7101. The linear correlations ($r^2 \geq 0.99$) between Sr isotope ratios and concentrations in waters collected during each single cruise indicates that such endmember variability has little effect on the binary mixing pattern of Sr in the MR mixing zone over short timescales, at least, over the few days of each sampling period.

3.1.2. Suspended particulate matter

There is no clear-cut relationship between particulate Sr concentrations and salinity. A majority of the Sr particulate data collected in this study fall within a narrow range, from 110 to 200 $\mu\text{g/g}$ (Table 2). There seem to be two salinity zones in which particulate Sr concentrations are at a maximum, regardless of the discharge and location. One of these zones is defined by moderate salinities of 12 to 17‰ (Fig. 4), within which samples collected from July 1999 and June 2002 have the highest particulate Sr concentrations. The other zone is characterized by salinities of about 5‰. Cruises from July 1999, March 2001 (MR and AR), and June 2002 contain samples with relatively higher particulate Sr concentrations at this salinity (Fig. 4).

3.2. Temporal variations of Sr in MR water

In monthly measurements of MR water at New Orleans, seasonal variations in both Sr concentration and isotopic composition are observed (Fig. 5a). The values range from 1.8 to 2.9 $\mu\text{mol/kg}$ for the Sr concentration and from 0.70966 to 0.71003 for the $^{87}\text{Sr}/^{86}\text{Sr}$ isotope ratio. The highest $^{87}\text{Sr}/^{86}\text{Sr}$ ratio and the lowest Sr concentration occur during high water discharge in the spring, although the correlation is weak ($r^2=0.41$). Generally, with increases in water discharge, there are decreases in dissolved Sr concentrations.

Our temporal analysis reveals that the Sr content of particulates co-varies with discharge from January until August (Fig. 5b and c). The enhanced discharge during spring led to increased suspended particulate matter (SPM) concentrations and Sr concentration of the particulates. However, during early fall (October), as variations in SPM content continued to follow changes in discharge, the Sr concentration of the particulates increased dramatically. Indeed, maximum Sr concentrations of the particulates in October are almost double those measured in April during highest discharge. Note, however, that the content of Sr associated with the particulates in the water is low (open triangles; Fig. 5c) due to the low concentration of total SPM.

4. Discussion

Sr in MR water mixes with GOM seawater Sr in a generally conservative manner (Fig. 3a and b). There are minimal deviations from a purely conservative behavior, but these deviations are measurable, and are likely due to biogeochemical processing in the estuary. In the following sections, we address the causes of and implications for this minimal non-conservative behavior.

4.1. Variations in the river input of Sr

Temporal variations in the Sr concentration and the $^{87}\text{Sr}/^{86}\text{Sr}$ isotope ratio of MR water (Fig. 5a) modify the amount and isotopic composition of Sr that mixes with GOM seawater. This variability in the riverine endmember over seasonal timescales produces the major scatter observed in the Sr isotope mixing diagram (Fig. 3b).

Changes in the relative contributions of upstream tributaries are likely a main cause for the observed temporal variations in both Sr concentration and $^{87}\text{Sr}/^{86}\text{Sr}$ ratio (Fig. 5a) of the lower MR. In general, the Sr concentration and isotopic composition of rivers are a function of the lithology of the drainage basin (Wadleigh et al., 1985; Aberg and Wickman, 1987; Albarede and Michard, 1987). The MR drainage basin encompasses 45% of the contiguous United States. Each part of the basin, through which the various tributaries flow, is composed of various geologic terrains. For this reason, each tributary likely has different Sr isotope systematics. Indeed, as observed by Goldstein and Jacobsen (1987), the upper MR (at Chester) has a Sr concentration of 3.0 $\mu\text{mol/kg}$ and a $^{87}\text{Sr}/^{86}\text{Sr}$ isotope ratio of 0.70953, the Ohio River has a Sr concentration of about 2.2 $\mu\text{mol/kg}$ and a $^{87}\text{Sr}/^{86}\text{Sr}$ isotope ratio of 0.71106 ± 10 , and the Tennessee River has a Sr concentration of 0.6 $\mu\text{mol/kg}$ and a Sr isotopic ratio of 0.71123 ± 7 (Goldstein and Jacobsen, 1987). Nearly 90% of the water discharged to the GOM comes from the Ohio River and upper streams of the MR (including the Missouri River), among which the Ohio River system (including the Tennessee River) alone contributes $\sim 50\%$ of the total (Meade, 1996). In 2000, the importance of the Ohio River with respect to lower MR discharge was extraordinary during the spring high discharge period, though less so during other seasons in which the upper MR tributaries played a comparable or more important role (discharge comparison made using data from <http://waterdata.usgus.gov>). Given the lower concentration and higher isotopic ratio of Sr in the Ohio River (Goldstein and Jacobsen, 1987), we believe that

the highest Sr isotope ratio and lowest Sr concentration observed during the highest discharge in the lower MR (Fig. 5a) was the result of a significant contribution from the Ohio River. The relative contribution from a tributary to the Sr variability in the lower MR may not be simply proportional to the tributary's discharge percentage in the lower MR. As suggested by Aubert et al. (2002), even in a catchment with a single type of bedrock lithology, Sr isotopic ratios of streams can change with fluctuations in discharge. High stream discharge may release more radiogenic Sr by leaching deeper layers of soils, which have been found to be more radiogenic in Sr (Aubert et al., 2002).

Our monthly sampling analysis reveals that the Sr concentration of the dissolved pool is correlated negatively with water discharge ($r^2=0.66$). However, the flux of Sr in the dissolved pool is positively correlated with water discharge ($r^2=0.92$), i.e., higher water flow delivers more Sr to the Gulf of the Mexico. This is not surprising given that the Sr concentration in the river does not vary by much. Nevertheless, a linear regression analysis of the Sr flux versus water discharge yields the following relationship:

$$\begin{aligned} \text{Sr flux}(\text{g a}^{-1}) &= 1.32(\pm 0.13) \times 10^8 \\ &\times \text{discharge}(\text{km}^3 \text{ a}^{-1}) \\ &+ 1.72(\pm 0.51) \times 10^{10} \end{aligned}$$

Using a decadal (1993–2002) mean annual average discharge value at Tarbert Landing in MS ($450 \text{ km}^3 \text{ a}^{-1}$; average of US Army Corps of Engineers website data: <http://www.mvn.usace.army.mil/eng/edhd/watercon.htm>), one can calculate an average Sr flux over this period of $7.7(\pm 1.1) \times 10^{10} \text{ (g a}^{-1})$.

4.2. Sr variations in the mixing zone

For the most part, Sr isotope ratios display typical conservative behavior within the mixing zone. However for samples from July 1999 that have salinities between 15 and 20‰ (circled in Fig. 3c), the Sr isotope ratios lie above, and outside the error of, any conceivable mixing line between GOM seawater and MR endmembers (Fig. 3c). Note that two of the four anomalous samples have been duplicated (from scratch, at separate institutions—see Section 2) with respect to their Sr isotopic composition suggesting a reproducibility that is better than 0.001%. A third source needs to be invoked to explain the radiogenic Sr anomalies in Fig. 3c. Potential candidates for this third source include: 1) submarine groundwater that is enriched in radiogenic Sr and discharged into the GOM, 2) radiogenic particulate

Sr that is dissolved and released into the mixing zone, and 3) greater concentration of radiogenic colloidal organic and/or inorganic particles. We have little data which strongly support any of these processes, and, therefore, can only list these hypotheses here.

However, there is some data which supports process #2, i.e., adsorption–desorption processes between particulate and dissolved Sr do seem to play a role in the mixing zone. High-salinity samples from the low-discharge November 2001 cruise have Sr concentrations that are lower than what is expected for conservative mixing (Fig. 3a). Indeed, high-salinity samples (i.e., 35‰) have Sr concentrations of about $83 \mu\text{mol/kg}$, about 8% lower than the accepted seawater value of $90 \mu\text{mol/kg}$. This difference is twice as high as the analytical error for the high-salinity samples (Section 2) and, therefore, statistically significant. Lower-than-expected Sr concentrations during times of low discharge may be due to adsorption of dissolved Sr onto particles. Adsorption of Sr onto Fe–Mn oxyhydroxide particulates has been observed by Andersson et al. (1994) in the Baltic Sea. There is some evidence of increased particulate Sr concentrations at salinities of 35‰ (Fig. 4), although the extent of the increase is less than that observed at $\sim 5\%$ and $\sim 12\%$ salinities (Fig. 4).

4.3. Implications for oceanic Sr budget and Sr isotope correlative techniques

As has been noted by many researchers, a single measurement of an element in a river is not adequate for mass flow estimates, especially in a river like the MR that has strong seasonal variability in its hydrological conditions. Among the factors that influence the Sr input from the MR to the GOM, river discharge appears to play the most important role. During the period of this study (July 1999 to June 2002), the water discharge of the MR varied from 120 to $1000 \text{ km}^3 \text{ a}^{-1}$. Based on the flux-discharge equation (see Section 4.3), such a significant variability in discharge implies that the annual Sr flux from the MR to the GOM changes between about $3.8 \times 10^{10} \text{ g a}^{-1}$ and $14 \times 10^{10} \text{ g a}^{-1}$. Hence, in the case of the MR, there is a good chance that one may over- or under-estimate the Sr flux based on a single measurement. For large rivers (e.g. Ganga–Brahmaputra river system) that have Sr isotopic compositions that are distinct from that of the open ocean, significant errors in estimating the Sr flux can be problematic to the Sr isotope mass balances of the ocean which, in turn, can hamper interpretations of the relative importance of changes in riverine sources to the ocean and weathering, and, hence, climate.

The modification of the fluvial Sr flux by non-conservative effects in the MR estuary is minor. The small, but measurable, anomalies in both Sr concentration and isotopic ratio are likely caused by the weak non-conservative behavior of Sr, and can occur in both brackish water and seawater influenced by the river plume at coastal margins. The Sr isotopic anomalies, i.e., deviations from conservative behavior, are small and within about 40 ppm.

5. Conclusion

The input of Sr from the MR to the GOM varies significantly in both flux and isotopic composition. There is significant hydrological control on the river-borne Sr flux to the ocean, which suggests that an estimate of Sr flux on the basis of a single sample is not adequate to reveal a mean input on annual, decadal, or longer time scales. There is limited non-conservative behavior of Sr in the mixing zone of the MR. This behavior may be due to redistribution of Sr between dissolved and particulate phases, changes in the quantity and/or composition of colloidal material which may include both organic and inorganic components, and/or supply of Sr by submarine groundwater discharge. The extent of the non-conservative geochemical behavior of Sr does not compromise the use of Sr isotope ratios for stratigraphic dating purposes.

Acknowledgements

We thank Tom Bianchi, Brent McKee, Mike Dagg and Pete Swarzenski for inviting us to join the various cruises from which much of the data in this paper were obtained. We are grateful to Lui-Heung Chan, Brent McKee and Tom Bianchi for valuable discussions and comments on the manuscript. We thank Michael Bizimis, Afi Sachikocher, Vincent Salters, Leroy Odom and Xin Li at FSU, and Lui-Heung Chan and Thomas Blanchard at LSU for help in measuring Sr isotope ratios. We are grateful to two anonymous reviewers for constructive reviews. This research has been funded by the Tulane-Xavier Center for Bioenvironmental Research and the LEAG (NOAA-USGS) program.

References

- Aberg, F., Wickman, F.E., 1987. Variations of $^{87}\text{Sr}/^{86}\text{Sr}$ in water from streams discharging into the Bothnian Bay, Baltic Sea. *Nordic Hydrology* 18, 33–42.
- Albarede, F., Michard, A., 1987. Evidence for slowly changing $^{87}\text{Sr}/^{86}\text{Sr}$ in runoff from freshwater limestones of southern France. *Chemical Geology* 64, 55–65.
- Andersson, P.S., Wasseerburg, G.J., Ingri, J., Stordal, M.C., 1994. Strontium, dissolved particulate loads in fresh and brackish waters: the Baltic Sea and Mississippi Delta. *Earth and Planetary Science Letters* 124, 195–210.
- Aubert, D., Probst, A., Stille, P., Viville, D., 2002. Evidence of hydrological control of Sr behavior in stream water (Strengbach catchment, Vosges mountains, France). *Applied Geochemistry* 17, 285–300.
- Brass, G.W., 1976. The variation of the marine $^{87}\text{Sr}/^{86}\text{Sr}$ ratio during Phanerozoic time: interpretation using a flux model. *Geochimica et Cosmochimica Acta* 40, 721–730.
- Burke, W.H., Denison, R.E., et al., 1982. Variation of seawater $^{87}\text{Sr}/^{86}\text{Sr}$ throughout Phanerozoic time. *Geology* 10, 516–519.
- Capo, R.C., DePaolo, D.J., 1990. Seawater strontium isotopic variations from 2.5 million years ago to the present. *Science* 249, 51–54.
- Coleman, J.M., Roberts, H.H., Stone, G.W., 1998. Mississippi River Delta: an overview. *Journal of Coastal Research* 14 (3), 698–716.
- Denison, R.E., Koepnick, R.B., Burke, W.H., Hetherington, E.A., 1998. Construction of the Cambrian and Ordovician seawater $^{87}\text{Sr}/^{86}\text{Sr}$ curve. *Chemical Geology* 152, 325–340.
- Derry, L.A., France-Lanord, C., 1996. Neogene Himalayan weathering history and river $^{87}\text{Sr}/^{86}\text{Sr}$: impact on the marine Sr record. *Earth and Planetary Science Letters* 142, 59–74.
- de Villiers, S., 1999. Seawater strontium and Sr/Ca variability in the Atlantic and Pacific oceans. *Earth and Planetary Science Letters* 171, 623–634.
- Edmond, J.M., 1992. Himalayan tectonics, weathering processes, and the strontium isotope record in marine limestones. *Science* 258, 1594–1597.
- Goldstein, S.J., Jacobsen, S.B., 1987. The Nd and Sr isotopic systematics of river-water dissolved material: implications for the sources of Nd and Sr in seawater. *Chemical Geology. Isotope Geoscience Section* 66, 245–272.
- Harris, N., Bickle, M., Chapman, H., Fairchild, I., Bunbury, J., 1998. The significance of Himalayan rivers for silicate weathering rates: evidence from the Bhote Kosi tributary. *Chemical Geology* 144, 205–220.
- Henderson, G.M., Martel, D.J., O’Nions, R.K., Shackleton, N.J., 1994. Evolution of seawater $^{87}\text{Sr}/^{86}\text{Sr}$ over the last 400 ka: the absence of glacial / interglacial cycles. *Earth and Planetary Science Letters* 128, 643–651.
- Huh, Y., Edmond, J.M., 1998. On the interpretation of the oceanic variations in $^{87}\text{Sr}/^{86}\text{Sr}$ as recorded in marine limestones. *Proceedings of the Indian Academy of Sciences. Earth and Planetary Sciences* 107 (4), 293–305.
- McArthur, J.M., 1991. Stratigraphy with strontium isotopes. *Geology Today* 7 (6), 5i–5iv.
- McArthur, J.M., 1994. Recent trends in strontium isotope stratigraphy. *Terra Nova* 6, 331–358.
- McKenzie, J.A., Hodell, D.A., Mueller, P.A., Muller, D.W., 1988. Application of strontium isotopes to late Miocene–early Pliocene stratigraphy. *Geology* 16, 1022–1025.
- Meade, R.H., 1996. River-sediment inputs to major deltas. In: Milliman, J.D., Haq, B.U. (Eds.), *Sea-Level Rise and Coastal Subsidence: Causes, Consequences, and Strategies*. Kluwer Academic Publishers.
- Palmer, M.R., Edmond, J.M., 1989. The strontium isotope budget of the modern ocean. *Earth and Planetary Science Letters* 92, 11–26.
- Patterson, R.T., Blenkinsop, J., Cavazza, W., 1995. Planktic foraminiferal biostratigraphy and $^{87}\text{Sr}/^{86}\text{Sr}$ isotopic stratigraphy of the Oligocene-to-Pleistocene sedimentary sequence in the

- Southeastern Calabrian microplate, Southern Italy. *Journal of Paleontology* 69 (1), 7–20.
- Raymo, M.E., 1991. Geochemical evidence supporting T.C. Chamberlin's theory of glaciation. *Geology* 19, 344–347.
- Stoll, H.M., Shrag, D.P., 1998. Effects of quaternary sea level cycles on strontium in seawater. *Geochimica et Cosmochimica Acta* 62, 1107–1118.
- Vaiani, S.C., 2000. Testing the applicability of strontium isotope stratigraphy in marine to deltaic Pleistocene deposits: an example from the Lamone River Valley (Northern Italy). *Journal of Geology* 108 (5), 585.
- Veizer, J., Buhl, D., Diener, A., Ebner, S., Podlaha, O.G., et al., 1997. Strontium isotope stratigraphy: potential resolution and event correlation. *Palaeogeography, Palaeoclimatology, Palaeoecology* 132, 65–77.
- Wadleigh, M.A., Veizer, J., Brooks, C., 1985. Strontium and its isotopes in Canadian river: fluxes and global implications. *Geochimica et Cosmochimica Acta* 49, 1727–1736.
- Xu, Y., 2004. Strontium geochemistry in the estuarine mixing zone of the Mississippi River. PhD thesis, Tulane University, 124 p.